Wireless Personal Communications (2020) 115:203–237
https://doi.org/10.1007/s11277-020-07568-9

Polygon Based Topology Formation and Information Gathering in Satellite Based Wireless Sensor Network

Padmaja Kuruba[1] · **N. D. Dushyantha**[2]

Published online: 2 July 2020

Abstract
The satellite network is one of the major source of information and these days small satellites are gaining lot of focus. The group of small satellites form a distributed network that work collaboratively to accomplish the mission task. These networks are very similar to the terrestrial wireless sensor network in terms of restricted resources and constrained capabilities. Sometimes, network of small satellites is also called as space based wireless sensor network (SBWSN). In any distributed network, topology formation and its control plays a significant role. This is true for SBWSN also. The topology in SBWSN decides the area of coverage (field of view), time of coverage, data gathered and data transmitted to ground station. The proposed topology is a distributed network of small satellites formed by trivalent, toroidal and spherical polyhedron graph forming a fullerene, which is called as polygon based network topology (PBNT). It comprises of both pentagonal (F_p) and hexagonal (F_h) faces with K regular graphs such that $K \geq 3$ with genus equal to 1. It also satisfies Eulers formula with n vertices. The fullerene comprises of simple rings and each of this ring forms the cluster. Each cluster is further represented as a triangular grid, that is linearly convex or non-linear, with K-connected graph along with Hamiltonian extendible cycle. The nodes/satellites on the triangular grid represent sensing nodes (low capability nodes/satellites), while the vertices of the ring are sink nodes (higher capability nodes/satellites). In this work, the topology is formed by small satellites (pico or nano satellites). In the proposed topology formation, the network is considered as virtual network with logical neighbours forming the cluster. Each node in the cluster covers a particular swath for a particular time interval based on the mission payload and on the p3 tiling. In the simulation, we consider n small satellites being placed in low earth orbit (LEO), (where n ranges from 3 to 150). The performance enhancements are seen during simulation in the following parameters, (1) *Coverage Area*: The coverage area increases as multiple satellites have different field of view at different times. (2) *Reduces Gaps*:The proposed distributed network also minimises uncovered areas as multiple satellites cover the target location at different time stamp which is not possible by a single large satellite. (3) *Increase in Data Throughput*: Each satellite in the network transmits data, when it is at perigee. The data throughput of the network increases, as data is transmitted by multiple satellites. Therefore, the throughput is increased by n-fold. (4) *Continuous Connectivity*: The data captured by one satellite in the network is made available to other using multi-hop communication. Thus the proposed topology also increases the continuous connectivity between satellites and

Extended author information available on the last page of the article

also with the ground station. (5) *Increases lifetime and Network Reliability*: The SBWSN accomplishes its mission task even when one/more satellites encounters functional failure. The satellites in the network can reconfigure themselves and continue the mission task. Thus SBWSN also reduces the risk of mission failure and ensures mission reliability. Due to reconfiguration the lifetime of the network is also increased. The proposed topology is used for small satellites (specially nano and pico satellites) network, which permit the single board satellite weighing less than 10 kg (Pico satellite less than 1 kg and nano satellites less than 10 kg). The advantage of these small satellites network over single large satellite is low cost and reduced development time, as it uses commercially of the shelf (COTS) components. In this paper, we propose network architecture formed by the spherically embedded clusters formed by polyhedron. The vertices of polyhedron have both pentagonal (F_p) and hexagonal (F_h) faces with K regular graphs such that $K \geq 3$, with genus equal to 1. The vertices of these polyhedron form the sink nodes and the other nodes are sensing nodes. Here satellites and nodes are interchangeably used. Sensing nodes are used for data gathering (pico/nano), while sink nodes are higher capability nodes which perform computational extensive operations in the network (nano or macro satellites). The sensing and sink nodes transmit data to the ground station when they are at perigee. The main objective of the proposed work is, technology demonstration of low cost, distributed small satellites network for earth observations replacing single huge satellite.

Keywords Small satellite network · Topology formation · Data gathering

1 Introduction

Today 2/3rd of the world, still does not have the infrastructure for the Internet and terrestrial network are unable to cover large areas and long distances. The satellite network plays a vital role in wide area coverage with remote sensing and planetary exploration, where wired network is not possible. In the current generation, satellite network is a backbone for providing global coverage and broadband access to the users (real time and non-real time applications). The major applications of satellite network are earth observation, multimedia access, scientific observation and interplanetary exploration [1]. In the traditional satellite communication, single large satellite covers a particular area of the earth for a small duration and then transmits that information to the ground station when it is at perigee. The conventional single large satellite communication has challenges like, high cost, limited area of coverage, low data throughput, and reduced reliability and lifetime of the mission caused due to functional failure. To handle these problems in the network, a group of small satellites are used to form a distributed network that collaboratively work to accomplish the mission.

Due to recent technological advances, manufacturing of small satellites using the commercial off the shelf (COTS) components have reduced the development time considerably, while making it feasible technically and economically viable. The group of these small satellites collaboratively works to form a distributed network. In the recent years, many small satellites(nodes) collaborate (use the resources of the neighbouring nodes in the network) and function distributively to perform a common task [2–4]. This distributed structure of small satellite forms a sensor web known as Space based wireless sensor network (SWSN) which are similar to the terrestrial wireless sensor network (WSN) [5]. SWSN

are also called distributed space based wireless sensor network (DSBWSN). The similarity between the DSBWSN and WSN are that, both are the networks formed by small devices (nodes) with restricted capability that perform a specific task by coordination and collaboration. DSBWSN have resource constraints and limited capability similar to WSN. From the study, we see that DSBWSN and WSN share lot of common features.

DSBWSN is advantageous, as it provides higher spatial and temporal resolution. It also has smooth degradation to single satellite failure, which further increases the reliability of the network [1]. Along with the advantages, DSBWSN has few challenges like (1) topology formation (with nodes being heterogeneous or homogeneous), (2) determination of attitude, node distribution in each orbit, communication link between the nodes and to the ground station, (3) mobility of the nodes and its control mechanism, (4) data acquisition and flow control mechanism. Networks with pico and nano satellites become even more challenging as these have limited capabilities and constrained resources. These small satellites are generally a non-propulsion system [6] thus energy sustainability is a major issue. Thus topology formation is the fundamental requirement in DSBWSN for handling the resources efficiently. The topology in DSBWSN basically depends on the geometry of formation in a network. Geometry determines the effective communication between the satellites in the network for accomplishing the mission task with the available nodes in the network. The essential parameters which decide the topology of the network are number of satellites in the network, number of times satellite is at perigee, hardware capabilities of each satellite (especially antennas and on-board power and storage devices), line of sight (LOS), angle of elevation and space environment. Topology further decides the throughput of the system based on transmission window and coding schemes [7].

2 Related Works

Some of the well-known satellite networks are walker delta constellation, Molniya constellation, global positioning system (GPS), surrey disaster monitoring satellite network, Iridium satellite network, Globalstar, GLONASS, Teledesic, Multi-Synchronous Orbits ConStellation (MSOCOS), Juggler orbit constellation, Orbcomm etc [8].

The author [9] has referred to walker delta constellation as one of the most commonly used topology formation in satellite network. It is a LEO constellation with satellite orbits overlapping in opposite direction that depends on cross seam links for data propagation. There are two drawback in this constellation, it has small uncovered areas of geographical swath and communication latency is high as Inter-satellite link involves switching between higher altitudes during inter-satellite data communication.

The author [10] describes Molniya constellation used as an alternative to higher orbit satellites to cover the application area continuously being at lower orbit. These are deployed in LEO, but has high elliptical orbit for covering larger area continuously. The disadvantage is that the number of times it can transmit data to the ground station is limited. Hence the data throughput is considerably less.

GPS comprises of 24 satellites in the constellation used for navigation. The weight of each satellite is more than 1000 kg and is placed in Medium Earth Orit (MEO) at an altitude of 20,200 km. Out of 24 satellites, 21 are active satellites that are used for navigation and remaining three are spare satellites. These spare satellites are placed in the parking orbit to replace when any active satellite fails. These satellite constellations do not have a on-board control system for maintaining their position in the orbit and has to depend on

ground station for control operation. If more than 3 satllites fail, then the entire mission will be a failure [11–13].

From the survey of last 25 years, more than four thousand satellite launches are accomplished by various space players including Government agencies, private agencies and also under Universities programs. From the statistics we see a large number of mission failure. The root cause for failure are due to launch failure, functional failure and external environmental factors of space. Around 150 missions have failed due to functional failure of the satellite. Functional failures are from Attitude and Orbit Control System (AOCS), power subsystem, Command and data handling subsystem, mechanical subsystem, software failure etc. Large satellites failure causes a huge loss with respect to development time and mission cost [14].

Technological growth and research in distributed mission with small satellites have envision DSBWSN as propitious area for future low cost space mission. This has led to the development of small satellites that can replace large satellite, while accomplishing the mission goal with reduced development time and at lower cost. This has also led to the path for students to involve in space mission.

The idea of student satellite development (low cost, small size and lesser development time) started in University of Stanford. These small satellites were approximately less than a kilogram of weight, costed approx. $ 40–50 k with development time as 1.5–2 years and launch cost was below $ 35 k. During the initial times these were considered as secondary payload by the launcher, but in the recent times small satellite launcher are also being developed. The deployment of small satellites by space agencies (ISRO, NASA, ESA etc.) and Universities like Stanford, California Polytechnic, Shizuoka, Tokyo, Sergio Arboleda has demonstrated the technology viability of these small satellite network [4]. These features of small satellites has attracted many space researcher.

The author [15] describes the development of UWE-1 to demonstrate the capabilities of small satellites for telecommunication application and the UWE-2 for attitude determination in 2007. Many such missions like pico panther, picopanther II, string of pearls and cluster formation are used in polar or sun synchronous orbits for various applications.

The authors in [16], describe flower constellation, where the reference satellite is followed by 3-D space track, which theoretically proves the compatibility of dual compatible flower constellations with simultaneous synchronization. Increase in the coverage area compared to single satellite is demonstrated by this work. The flower constellations were extensively used for distributed computing in space network. The author in [17], describe the formation of the network using Harmonic flower constellation and lattice flower constellation (2D and 3D). The author provides a comparative study and the advancements of lattice and flower constellation. This topology of the network shows the average performance enhancement with respect to positioning accuracy over flower constellation.

The authors [18] says space domain is no longer in the hands of superpowers. The Consortium of UK, Turkey and Nigeria developed and launched Disaster Monitoring Constellation (DMC) using small satellites for earth observation. This mission was developed for human welfare. It also provides data for students and researchers for scientific exploration and development of new space applications. This consortium works in cooperation and reduces the risk of launch failure as each satellite is launched at different time. DMC helped daily imaging of earth surface with improved spatial resolution using efficient sensors having wide field-of-view with 32 m ground sample distance in three spectral bands. Though DMC works in coordination, but distributed computing and dynamic scheduling was not included in this mission. Researches prefer formation flying with on-board control

mechanism in DSBWSN for dynamic topology formation and reconfiguration during satellite failure.

Formation flying(FF) of satellites, is defined as the set of satellites having on-board control system. The relative positions of satellites in the formation is maintained using closed loop control mechanism [19]. There are various strategies used for formation flying namely (1) virtual structures, where the centralised planner is used for control operation to maintain the formation. (2) Other method of maintaining FF is by using behavioural strategies like swarm algorithms (Example: ANT colony, school of fish and flock of birds).

The author [20] in this paper addresses the first formation flying mission with Twin satellites working at a height of 500 km used for data collection of both static and time-varying gravitational field of the earth. This system has a complex AOCS along with K Band system and GPS to determine the position of the satellite required to determine the gravitational field. The mission had a gyro failure and the subsequent mission GRACE 1 demonstrated adaptation and graceful degradation during mission failure. This also proved to improve the lifetime of the mission.

The author in [19] describes the formation flying of swarm of three small satellites in three orbital planes. Two of the satellite have same inclination, while other have different inclination to provide drift-over time. In this paper we also see the AOCS accuracy within 5° accuracy.

The author in [21] uses a distributed network of small satellite that demonstrates the reconfiguration of the communication links between the nodes during reconfiguration of the nodes in the network. This reconfiguration uses ant colony optimization techniques to establish the communication links between the nodes [5, 22]. This proves that dynamic reconfiguration of the nodes in space is possible.

The author [23] in his work describes, the formation of the satellites using biological inspired swarm, that targets topology with collision avoidance. The mission adapts to dynamic reconfiguration, if the satellites in the formation drops below the threshold. The reconfigurable micro-satellites formation that uses active Radio frequency antennas with sparse aperture formation in AFRL mission is presented in the paper [24].

The author [25] describes, four models for Formation flying namely Ordinary Differential Equations expressed in terms of Cartesian coordinates (CODE), solution-based State Transition Matrix (STM) and Algebraic equations expressed in terms of Orbit Element Differences (OEDA). These models help in determining the topology of the network. They also predict the capability of increasing the network size based on the relative distances and the corresponding error index in the formation. Each of these models have different accuracy and different bit error rate for different relative distance between satellites in the network. If the mission requires less computation then OEDA is used as it takes less computation time to solve differential equations on board.

From literature survey we see a paradigm shift of using many small satellites (DSBWSN) instead from single large satellite. Some of the limitations of DSBWSN are topology of the network satellites, formation keeping, limited area of coverage, data throughput, network reliability, processing capabilities and stability of the network. The proposed work focuses on geometric framework in topology formation of small satellites that are stable and cover larger geographical area with higher throughput and reliability.

2.1 Our Contributions

The proposed topology is formed by trivalent, toroidal and spherical polyhedron graph forming a fullerene structure. This structure potentially comprises of both pentagonal and hexagonal rings with K regular graphs such that $K \geq 3$ with genus equal to 1. These ring structure forms the clusters. Each cluster is represented as a triangular grid that is linearly convex or non-linear using K-connected graph with Hamiltonian expendable cycle. The nodes on the triangular grid represent sensing nodes, while the vertices of the ring are sink nodes.

Our work differs from the existing work in the following ways (1) Modelling of network using trivalent, toroidal and spherical polyhedron graph forming a fullerene structure. (2) The rings of the fullerene structure forms clusters. (3) Modelling of the network as logical cluster in the virtual network. (4) The triangular grid is present within the cluster that is linear convex grid/non-linear convex grid with Hamiltonian cycles. (5) The network is employed with two levels of capturing/sensing the target by sensing nodes and sink nodes to increase the area of coverage. The network comprises of small satellites.

Some of the advantages of this network are (1) Covers small uncovered areas of geographical swath. (2) Improved area of coverage as both sensing nodes and sink nodes can gather and aggregate the information at different interval of time. (3) It has better throughput as each node can transmit the data at its perigee point. (4) Provide increased life time of the network. (5) Provide high reliability of the mission in-case of node failure. (6) Technically feasible and economical, due to usage of well tested commercial off the shelf components. (7) It requires less development time, with reduced mission cost.

Rest of the paper is organized as follows, Sect. 3 describes the proposed work comprising of network models, Sect. 4 describes the implementation of the proposed work, Sect. 5 describes the information gathering the life time of the network, Sect. 6 presents the simulations and result analysis and Sect. 7 finally concludes the work with the future scope.

3 Proposed Work

The satellite network in space, resemble mobile wireless sensor network (WSN) where the topology of the network dynamically changes with the mobility of the nodes. In this paper, we propose a polygon based network topology (PBNT), that is created using a spherical polyhedron structure with two or more regular polygons. The hexagon and pentagon are the regular polygon used in this polyhedron structure forming a fullerene. The PBNT structure has a minimum of threefold symmetric tiles, covering any small area without gaps or overlapping. This topology overcomes the drawback in [9]. The fullerene comprises of hexagonal/pentagonal structure. These structure forms the clusters and are represented using triangular grid as shown in the Fig. 1. The triangular grid is formed by line segment. These line segment represent the inclinations of the nodes in the network. The triangular grid is Hamiltonian with linear convex or non linear formation. The topology also satisfies the Hamiltonian extended cycle for scalability.

The network is considered to have logical cluster with logical neighbours. Though the nodes are mobile, logical neighbours in the network are well defined, as the mobility of the node is predefined by orbital elements. Thus logical neighbours at any given time are known to each other in the normal working condition. This reduces on-board computation to find its neighbour for every iteration (Fig. 2).

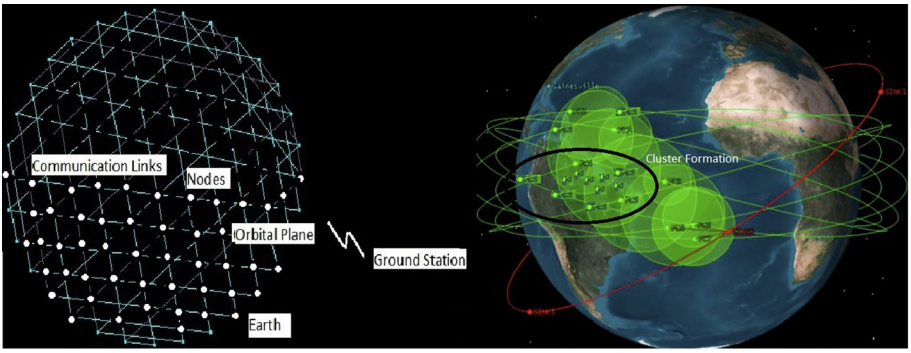

Fig. 1 SBWSN in space

The scheme of operation in proposed work is described in the following steps (1) The nodes are deployed in low earth orbit with altitude ranging from 550 to 1598 km. (2) The nodes are at same/different altitude with same or different inclination depending on the application. (3) The network topology is formed by polyhedron spherical structure. (4) Dynamic clusters are formed by the rings of the polyhedron structure forming logical clusters. (5) The network comprises of two types of nodes called as sensing nodes and sink nodes. (6) The vertex of the rings form the sink nodes/cluster heads. (7) Cluster heads/ Sink nodes are normally used for data transmission to ground station. (8) The topology determine the nodal period of the node in the network. This also determine the number of times the node is at the perigee and helps in data transfer to the ground station. (9) The edges connecting the nodes determines communication range which determines the size of polyhedron structure. (10) The area of coverage of the network is determined by orbital elements, the size of the cluster rings and the payload of the mission.

The performance of PBNT is simulated using LEO satellites, with sensing nodes weighing approximately 1 kg and sink nodes weighs between 1 and 10 kg. The performance parameters such as swath,throughput, energy consumption, lifetime and stability of the network is evaluated.

In this section, we describe the models of PBNT and logical cluster. This network model comprises of sensing and sink nodes that form network. It also describes covering a particular swath at particular period of time and transmitting using communication links, while maintaining the formation using control mechanisms. It demonstrates large

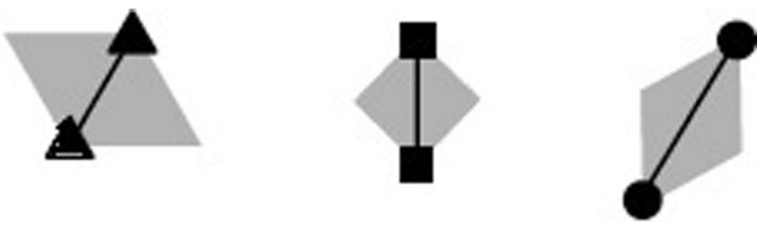

Fig. 2 Representation of inclination as line segment

area of coverage including small uncovered region that increases throughput and network lifetime.

3.1 Preliminaries

The symbolic notations used in the proposed works are given in the Table 1.

Table 1 Symbol notations

Symbols	Definitions
a	Semi major axis
e	Orbital eccentricity
ω	Argument of perigee
Ω	Ascending node longitude
$N_{sensing}$	Sensing node
$N_{isolated}$	Isolated node
N_{sink}	Sink node
$Cluster_n$	Cluster
ϕ_{nodei}	Satellite altitude
O_{nodei}	Orbital plane
I_{nodei}	Satellite inclination
PL	Left neighbouring node
PR	Right neighbouring node
PUL	Upper left neighbouring node
PUR	Upper right neighbouring node
PDL	Bottom left neighbouring node
PDR	Bottom right neighbouring node
G_{C_n}	Cluster depicting a subgraph
$C_{(rsink)}$	Swath of sink node
$C_{(rsensing)}$	Swath of sensing node
$C_{(Nodetime)}$	Coverage time
E_r	Earth radius
S_r	Satellite radius
$\mathfrak{R}_d$	Relative distance
Nei_{ij}	Logical neighbours
$\mathfrak{R}_C$	Communication range
E_{res}	Residual energy
Δ_{Ferr}	Formation error
Vec_u	Vector representation of along side edge of hexagon
Vec_v	Vector representation of center of hexagon
A_{Hexes}	Area of tiling
$Cluster_{Pn}$	Permutation of cluster formation

3.2 Proposed Model

This section presents network frame work, formed by spherical polyhedron graph with pentagonal or hexagonal rings forming clusters. It also explains the geometric structure of the cluster formation, which is the backbone in the proposed work.

3.2.1 Polyhedron Based Network Model

The distributed network in this work is formed by trivalent, toroidal, spherical polyhedron graph. This polyhedron graph further forms the fullerene comprising of both pentagonal and hexagonal faces. It is represented as a planar graph that is formed by a series of hexagon or pentagons.

Let us consider a graph with hexagons called as polyhex. Just for the purpose of representation we assume hexagons of same size, but in actual scenario the size of each hexagon(H) may vary based on the application. The polyhex is formed by H_n where $n = 1, 3, 4, 7, \ldots$ congruent hexagons. The skeleton of these polyhexes in planar graph with three fold tiling at the center is represented by black opaque dot, while the terminus is represented using a hallow circle. Figures 3 and 4 shows H_n for $n = 1, 3, 4, 7$. The center and the terminus helps in determining the formation of cluster required to cover a particular area of earth based on the application. Since dynamic topology formation is focused in this work, we use the concept of tiling for dynamic clustering. These polyhexes form the logical cluster.

The proposed topology is advantageous as it forms a network of embedded hexagon forming a scalable and re-usable network using existing space infrastructure.

3.2.2 Model for Logical Cluster Formation

The polyhedron or the fullerence topology comprises of rings that are either hexagonal or pentagonal structures. Each ring structure forms a cluster as shown in the Fig. 5 and is represented by Eq. 1.

$$H_n = C_1, C_2, C_3, C_4 \ldots C_n \tag{1}$$

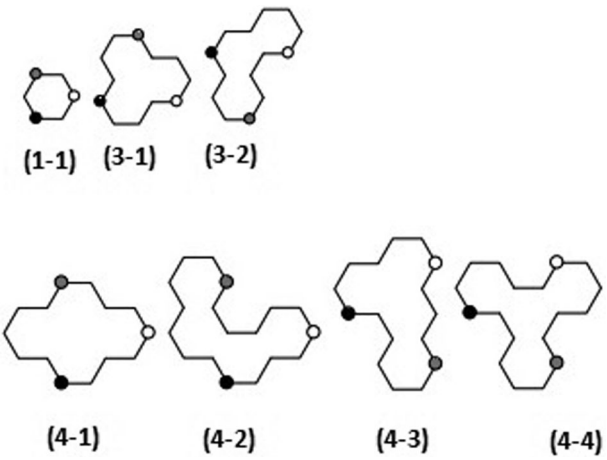

Fig. 3 Skeleton of polyhexes with its different inclination n – {1 – 4}

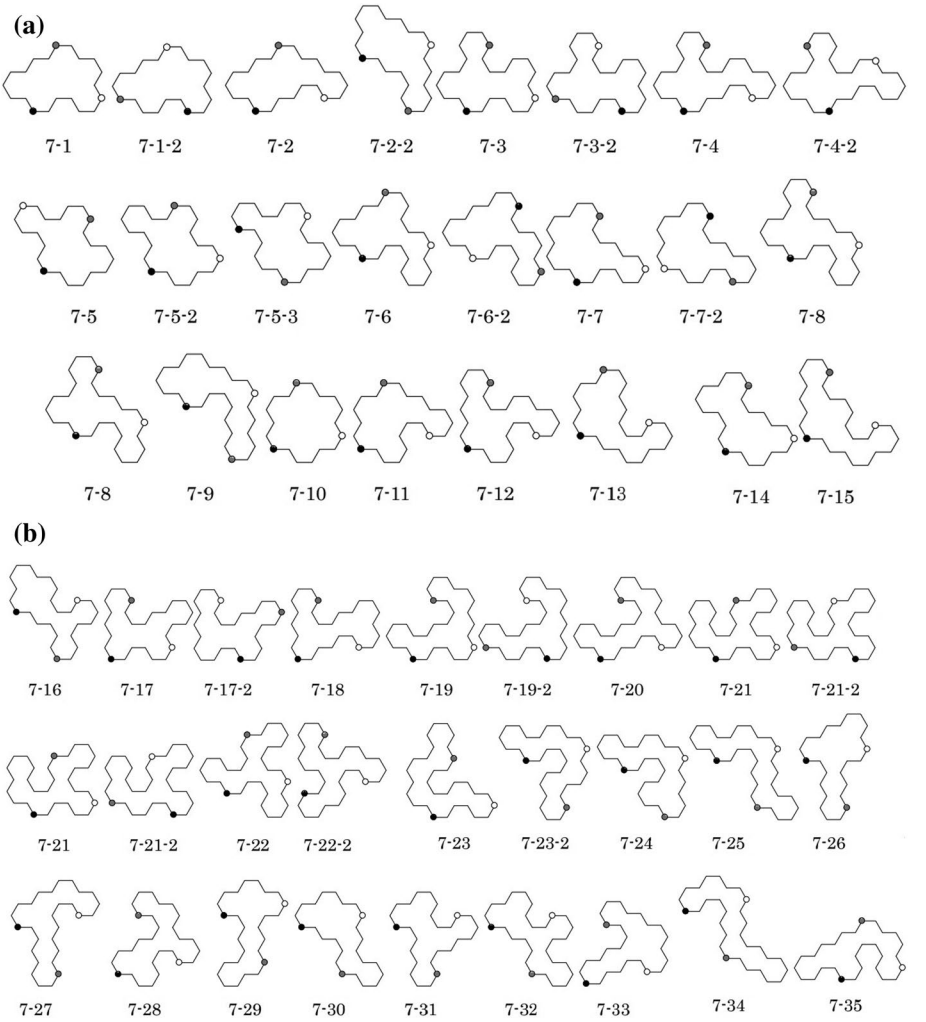

Fig. 4 Skeleton of polyhexes with its different inclination for n = 7

Fig. 5 Logical cluster formation

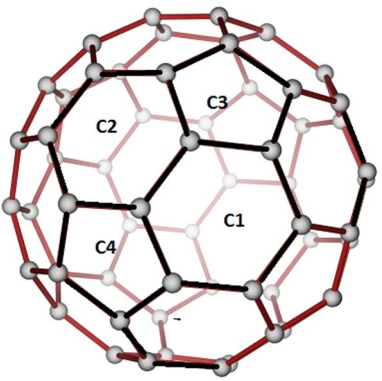

where C_i represent the cluster with $i = 1, 2, 3, 4 \ldots n$. The cluster formation is dynamic with the permutation of the nodes as shown in the Eq. 2.

$$Cluster_{P_n} = (0, \pm 1, \pm 3gm), ((\pm 1, \pm(2 + gm), \pm 2gm), (\pm 2, \pm(1 + 2gm), \pm gm) \quad (2)$$

where gm indicates the golden mean $((1 + \sqrt{5})/2)$ used for cluster formation based on the permutation of the nodes position in the network for a particular instant of time. The nodes lying within this region of the ring form the cluster members and the vertices of the ring are nominated as the cluster head as shown in the Fig. 5. The cluster are formed dynamically based on the mission application, number of nodes and the tiling/inclination of the nodes in the network. Tiling is a process in which congruent copies of one plane fill the other plane such that there are no overlaps. The symmetry of the group behaves as if tiling is transitive.

3.2.3 Formation of p3 Symmetry of Logical Cluster

Each of the ring is represented as a cluster in the polyhedron forming logical clusters. The logical cluster are formed using the tiling. Here tiling is considered with a basic unit as hexagon. The center to the terminus is represented using vectors (Vec_u, Vec_v) where Vec_u is along the edge and Vec_v is towards hexagon center as shown in the Fig. 6b. The polyhedron is created by the tiling of the hexagons to fit the skeleton of the network topology as shown in the Fig. 13a.

The algorithm used to form the hexagons in the cluster is as follows:

Algorithm 1 Proposed Scheme for PBNT

Select the origin and the terminus of the hexagon falling within the skeleton of the topology.

Select the unit hexagon with one edge common with the next.

Choose a area of this unit hexagon.

Make successive rotations till this unit shape(tiling) reach the terminus.

3.2.4 Triangular Grid Formation with p3 Symmetry Within the Cluster

The cluster if formed by triangular grid. This triangular grid is created by the tiling of the equilateral triangles that fit the polyhedron shape as shown in the Figs. 6b and 13a. The algorithm used to form the triangular grid is same as that of hexagon but the basic unit considered here is a equilateral triangle. The rotations of two, with a single triangle generates the entire tiling, forming a triangular grid. It also satisfies the p3 symmetry used for the skeleton of the network. The p3 tiling helps in covering the required area without any gaps in the network.

3.2.5 Area of Coverage by Cluster

Let (Vec_u, Vec_v) represent the vectors used to represent the unit triangle as shown in the Fig. 6b. The vector Vec_u is along the edge and Vec_v is towards unit triangle. The area constructed by these unit triangles is given by the Eq. 3 and the area covered by the hexagon cluster is given by the Eq. 4, where $(xVec_u, yVec_v) = \{1, 2, 3, \ldots\}$ are the scalar quantities used to reach to the terminus from center. In this case, as we consider the logical network,

Table 2 Orbital elements governing the topology formation

Orbital element	Relative expression
Semi-major axis	$a = \frac{\mu}{(\frac{2\mu}{P_r})-(v^2)}$
Eccentricity vector	$\vec{e} = \frac{1}{\mu}(nn - pp)$ where $pp = (\vec{v}\vec{P_r}).\vec{v}$ and $nn = \vec{P_r}[v^2 - (\frac{\mu}{P_r})]$
Inclination node in orbit	$i = cos^{-1}\left(\frac{(\vec{kk}.\vec{P_r}.\vec{v})}{\lvert\vec{P_r}.\vec{v}\rvert}\right)$
Argument of perigee	$\omega = \vec{e}.\frac{(\vec{ki})}{\lvert i\rvert}$
Ascending node longitude	$\Omega = cos^{-1}\left[\frac{x_n}{\frac{(\vec{ki})}{\lvert i\rvert}}\right]$

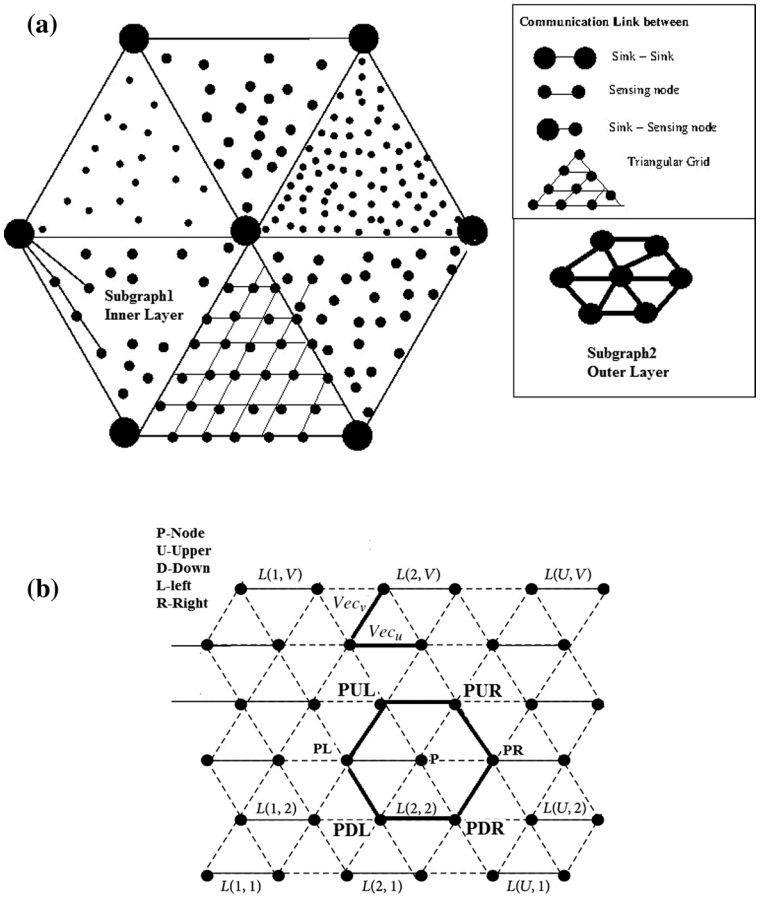

Fig. 6 **a** Geometrical framework of the PBTN and **b** triangular grid graph with neigbhour representation

the logical regions and the positions are synchronously switched to cover the region of the earth respectively.

$$A_{Tri} = 2\left((xVec_u)^2 + (yVec_v)^2 + xVec_u yVec_v\right) \tag{3}$$

$$A_{Hexes} = \frac{(xVec_u)^2 + (yVec_v)^2 + xVec_u yVec_v}{3} \tag{4}$$

3.3 Determination of Nodes Position During Dynamic Cluster Formation

In the proposed topology, we assume sun synchronous nodes as it takes the advantages of regular light in the orbit, due to constant angle between sun and the orbital plane. Other important factors that govern the topology formation are the orbital elements. The orbital elements determine the shape, size and position of the node in the orbit. Table 2 describe the orbital elements.

The position of the node in space is determined by the mean anomaly M_A given by the Eq. 5.

$$M_A = M_{A_0} + M_{motion}(t - t_0) + \delta P \tag{5}$$

where M_A is mean anomaly, M_{A_0} is initial mean anomaly at time t_0, M_{motion} is the mean motion which is a function of semi-major axis and elapsed time. $(t - t_0)$ indicates the time elapsed from the initial position to the current position, that is also subjected to δP which indicates perturbations caused due to J_2, J_3 and J_4. Mean anomaly is used to know the amount of time taken for the node to travel from one position to other position in the orbit. This determines the position of the nodes in the network. The position of the node at any given point of time is a function of (r, ϕ, θ) and is given by the Eq. 6–9

$$Sat_{pos} = f(r, \phi, \theta); \tag{6}$$

$$r = \frac{a(1 - e^2)}{1 + ecos(v)} \tag{7}$$

$$\theta = sin^{-1}(sin(v) * sin(i)) \tag{8}$$

$$\phi = sin^{-1} * \frac{tan(\theta)}{tan(i)} \tag{9}$$

where i indicates inclination, θ is the latitude of the node in the orbit, v is the true mean anomaly and ϕ is the meridian from the reference frame.

The position of the node with $\overrightarrow{P_r}$ representing the position of node and $|P_r|$ is the magnitude with Cartesian coordinates (x, y, z) as shown in the Eqs. 10–14

$$x = r(cos(\theta)cos(\phi)) \tag{10}$$

$$y = r(cos(\theta)sin(\phi)) \tag{11}$$

$$z = rsin(\phi) \tag{12}$$

$$\overrightarrow{P_r} = x(t)\vec{i} + y(t)\vec{j} + z(t)\vec{t} \tag{13}$$

$$|P_r| = \sqrt{x^2 + y^2 + z^2} \tag{14}$$

The measurement of position vector is also effected by the J_2 perturbation. The value of $J_2 = 0.0010827$ and the velocity vector is obtained using Runge Kutta method using 4th order. Thus the position of the node helps the dynamic formation of cluster and further increases the throughput and life time of the network due to collaborative work.

Dynamic clustering is formed based on the position of the nodes and the communication link, if it satisfies the Eq. 15. Here threshold includes position of the nodes in close proximity, velocity, perturbations, energy level of the node to participate in the cluster formation, communication link capabilities, security issues and application area.

$$Cluster_n = C_1, C_2, C_3, C_4 \ldots C_n \geq T_{hreshold} \tag{15}$$

The topology and the cluster formation is not strictly bound by exact values. The small variation in formation is the difference between measured and the reference positions is known as formation error. In the proposed work AFF sensor is used for finding the relative measurements. This error is corrected using algorithms with the support of gyros. Cluster head can also act as a reference for the neighbouring nodes to determine their relative distance and calculate the error.

3.3.1 Formation Factor

Maximum error permissible in the topology for the nodes to be within the formation is called as formation factor. The topology is chosen such that the formation factor is within the permissible range of application. The topology of the network can be periodically monitored by checking deviation in the distance or volume of the shape from the initial design. Later the current distance/volume is compared with the reference node. If the relative distance/volume is well within the expected range of the mission, then no control mechanism is used, else altitude determination and control system is used to maintain the topology of the network. This is a typical scenario where decentralized controlling mechanism is used to maintain the network in formations where nodes jointly accomplishes the task. The nodes here are coupled by task which require the topology to be intact. The permissible formation factor is given by Eq. 16

$$Formation/Error = \frac{Current\ Volume\ or\ Distance}{Reference\ Volume\ or\ Distance}\Delta_{Ferr} = \frac{V(x)}{V(ref)} \tag{16}$$

$$\Delta_{Ferr} = \begin{cases} No\ change & \text{if } (\Delta_{Ferr} \leq V_{Threshold}), \\ Allign\ nodes & \text{Otherwise} \end{cases} \tag{17}$$

4 PBNT Implementation Using Graph theory

A common way to model a network is by using graph. In the proposed topology, we define a undirected graph G constructed using the set of vertices and edges as shown in the Eq. 18. The vertices are assumed to be as nodes. The arc joining the two nodes is called edges and these edges in the graph represent the communication links. These link are used for data transfer from one node to the other. It is assumed that the logical neighbours are in line of sight and within the communication range required for information gathering.

$$G = \{E, V\} \tag{18}$$

$E(G)$ represent set of edges and $V(G)$ represent set of vertices. The network is considered as logical network with neighbouring nodes always in close proximity and within the permissible range of communication. The inter satellite link (ISL) are used as the arc connecting the nodes used for communication between the nodes. Figure 6a shows two types of nodes namely (1) sensing nodes $\left(N_{sensing}\right)$ and (2) sink nodes $\left(N_{sink}\right)$. Here small satellites like pico/nano satellites can be considered as $N_{sensing}$ nodes and nano/macro satellites as N_{sink} nodes. All $N_{sensing}$ nodes and all N_{sink} nodes are assumed to be identical and having the same functionality respectively. If the nodes are out of coverage area or failed due to energy draining or due to functional failure, such nodes are called isolated nodes represented as $N_{isolated}$. Incase of node failure or out of coverage, then the topology dynamically changes based on the available nodes. This ensures reliability of the network, which is a key aspect in DSBWSN.

The geometric framework of PBNT is shown in the Fig. 6a. The PBNT is a distributed network that comprises two layers forming logical network. The inner layer represent subgraph $G1$ and the outer layer represent subgraph $G2$ and $G = \{G1, G2\}$. The vertices of the inner graph hold $N_{sensing}$ nodes, while the vertices of outer graph holds N_{sink} nodes as shown in Fig. 6a.

4.1 Logical Cluster Formation

The Graph G has $N_{sensing}$ nodes in the network such that $N_{sensing}$ nodes > 2. The possible combination of cluster formation depends on the orbital elements of the nodes in the network. The nodes of the network are said to be locally connected, if each vertex of the graph is connected to the other vertex in G. Any two nodes in the network (x, y) with disjoint paths and each vertex $G(x)$ has $N(x)$ neighbouring vertices adjacent to X that can form disjoint hamiltonion cycles, iff the set of vertices $X \subseteq G$ [26–28]. The graphs with cycles is well suited for dynamic topology, that adapts themselves for node addition/deletion during node failure. The graph further can be represented as a triangle with these vertices as shown in the Fig. 7. These nodes are said to be connected locally.

A minimum of two nodes should be connected in the network to satisfy the distributed network. Every vertex of graph has a minimum degree of 2 and lies on the triangular grid of the graph. It also shows the possible neighbours in the network, which is represented as $L(U, V)$ as shown in the Fig. 6b where $U = \{0, 1, 2, \ldots\}$ and $V = \{0, 1, 2, \ldots\}$. Figure 6b shows the vertex PL, PR, PUL, PUR, PDL, PDR that forms a neighbouring nodes in the triangular grid graph, which are also called as sub-graphs of the Graph G and these vertices are positive integer values. The order and the bandwidth of this graph is $X + 1$. The vertices (sink nodes) of triangle form the outer layer of locally connecting nodes in the triangular grid graph. The nodes inside triangle are the sensing nodes used for sensing

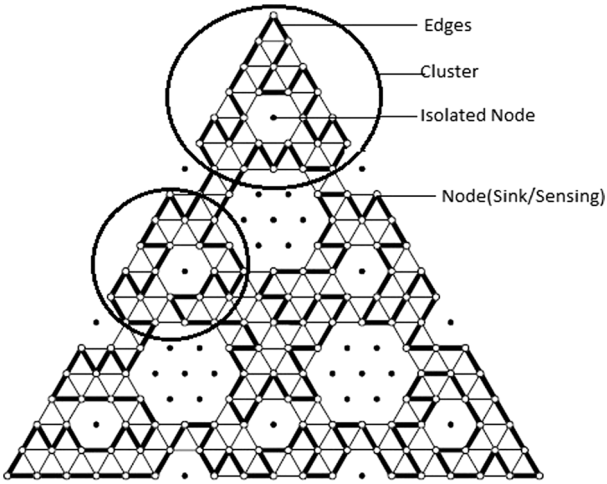

Fig. 7 Flow diagram of dynamic cluster formation in polygon based topology formation

based on the application. One complexity with this permutation of nodes getting connected depends on the permutation of nodes and the time complexity for this is given by O(N*N). The path selected for connectivity between the two nodes depends on the search for nearest neighbour. The triangular grid is formed with k-paths and k-cycles. The neighbouring nodes connectivity in the graph G can be isomorphic or cycle extendible. The graph is further divided into number of triangular grid graph obtained by intersection of grid lines (vertex) and line segments as shown in the Fig. 6b which forms logical clusters C_n. These clusters forms sub-graph such that $G_{C_n} \subset$ of G. The number of nodes in $G_{C_n} >= 3$.

One of the important concept of the PBNT is the formation of clusters. The proposed topology described has two layers, represented by sink graph and sensing graph. Let $G1 = (V_{(sink)}, E_{(sink)})$ represent a graph formed by the sink nodes that are higher capability nodes with higher communication range. $G2 = (V_{(node)}, E_{(node)})$ is a secondary graph with sensing nodes that are lower capability nodes and have lesser communication range. These sensing nodes are bidirectional graphs.

The PBNT uses skeleton of polyhexes with different inclinations to form dynamic and virtual cluster with logical neighbors. The cluster formation is based on the network parameters like communication range, area of coverage and energy of the nodes. The connectivity in PBNT is defined by the icosahedral structure that is similar to the fullerenes of carbon atoms. These fullerenes are structure of carbon atoms formed using hexagonal rings. These rings define the clusters, based on the connectivity and the strength of communication links. The communication protocols used for SBWSN are TCP/IP with few modifications to meet the space environment.

4.2 Communication Links in PBNT

In our work, the topology is dynamic in nature and hence the communication links between the satellites follow the logical connection between the two nodes. PBNT consists of communication links

- Between the sensing nodes as shown in matrix (22)
- Between sink to sink as shown in matrix (23)

- Between sensing node to sink node as shown in matrix (24)
- Between cluster heads as shown in matrix (25)
- Between sink to cluster head as shown in matrix (26)

Here matrix A in matrix (19) depicts the sensing nodes in the cluster while the matrix B matrix (20) are the sink nodes and Matrix (25) are the cluster heads in PBNT. The possible communication links between the nodes is given by the Kronecker product as shown in the matrix (22–24). If the nodes are not available then such nodes in the matrix are considered as isolated nodes. In other words we can say that the distance doesn't satisfy the required threshold. The weights are given to the links and the weight for non existing or isolated node is given as infinity.

A (*Sensing nodes*) are the sensing nodes in the SBWSN given by Matrix (20)

$$A(Sensing\ nodes) = \begin{bmatrix} a1 \\ a2 \\ a3 \\ \vdots \\ am \end{bmatrix} \tag{19}$$

B (*Sink Nodes*) are sink nodes in the SBWSN given by Matrix 20

$$B(Sink\ Nodes) = \begin{bmatrix} b1 & b2 & b3 & \vdots & bn \end{bmatrix} \tag{20}$$

C (*ClusterHeads*) are the cluster head in the SBWSN given by Matrix21

$$C(ClusterHeads) = \begin{bmatrix} c1 \\ c2 \\ c3 \\ \vdots \\ cm \end{bmatrix} \tag{21}$$

D_{SS} are the communication link and corresponding distance between sensing nodes given by Matrix 22

$$D_{SS}(Distance\ Between\ Sensing\ Nodes) = \begin{bmatrix} a11 & a12 & \cdots & a1q \\ a21 & a22 & \cdots & a2q \\ a31 & a32 & \cdots & a3q \\ \vdots & \vdots & \vdots & \vdots \\ am1 & am2 & \cdots & mq \end{bmatrix} \tag{22}$$

D_{SinkN} shows the communication link and corresponding distance between sink nodes given by the matrix 23

$$D_{SinkN}(Distance\ Between\ Sink\ Nodes) = \begin{bmatrix} b11 & b12 & \cdots & b1p \\ b21 & b22 & \cdots & b2p \\ b31 & b32 & \cdots & b3p \\ \vdots & \vdots & \vdots & \vdots \\ bn1 & bn2 & \cdots & bnp \end{bmatrix} \tag{23}$$

$D_{SenSink}$ shows the communication link and corresponding distance between sensing nodes and sink nodes given by the matrix 24.

$$D_{SenSink} = \begin{bmatrix} a11b11 & a12b11 \cdots & a1nb11 & \\ a11b21 & a12b12 \cdots & a1nb12 & \\ \vdots & \vdots & \vdots & \vdots \\ a11bm1 & a12bm2 \cdots & a1nbmn & \end{bmatrix} \tag{24}$$

D_{CH} are the connection and the Weights (distance) between cluster heads given by the Matrix 25

$$D_{CHs} = \begin{bmatrix} c11 & c12 & \cdots & c1p \\ c21 & c22 & \cdots & c2p \\ c31 & c32 & \cdots & c3p \\ \vdots & \vdots & \vdots & \vdots \\ cn1 & cn2 & \cdots & cnp \end{bmatrix} \tag{25}$$

$D_{SinkandCH}$ shows the connection and the Weights (distance) between sink nodes and cluster heads given by the Matrix 26

$$D_{SinkandCH} = \begin{bmatrix} c11b11 & c12b11 \cdots & c1nb11 & \\ c11b21 & c12b12 \cdots & c1nb12 & \\ \vdots & \vdots & \vdots & \vdots \\ c11bm1 & c12bm2 \cdots & c1nbmn & \end{bmatrix} \tag{26}$$

These weights determine the possible clusters, the grouping of sensing nodes in the cluster and also the cluster head. Cluster head and the sink node is chosen which is near to maximum nodes in the cluster.

4.2.1 Control Mechanism

The concept of cluster formation has gradually replaced the centralized control as seen in constellation of satellites. It helps in decentralized and automatic control mechanisms that further reduces the mission cost. The cluster formation takes the advantage of active control mechanism (ACM) which involves rigid control of nodes in the network. The ACM uses on-board, algorithms based on relative position measurement in the orbit. It becomes a real time control mechanism for tightly holding the formation in space. The cluster formation and its control mechanism is explained in the flow diagram Fig. 7. The above matrices help us in determining the deviation from the current and reference position. The correction factor is estimated. This is a software driven correction method. There are various sensors used to determine the relative distance between the nodes which can be as precise as $\mp$ 10 nm using AFF sensor or laser. So it depends on the application to use software or hardware control mechanism for formation flying.

4.2.2 Communication Range

The communication range of the network depends on the relative distance between the nodes, orbital plane, inclination and line of sight between the transmitter and the receiver. Each of the node is placed at a certain position $x_i = \{\phi_{nodei}, O_{nodei}, I_{nodei}\}$, where $\{\phi_{nodei}, O_{nodei}, I_{nodei}\}$ indicate the altitude of the satellite, orbital plane and inclination of the orbit respectively. The relative distance $\mathfrak{R}_d$ between the two nodes is given by Eq. 27 and node i and j are said to be logical neighbours (Nei_{ij}) only if $\mathfrak{R}_d$ is within communication range $\mathfrak{R}_C$. Sensors like AFF sensor or laser are used to determine the relative distance between the nodes with precision

of ∓ 10 nm. Communication range includes LOS or Multihop communication. For multi-hop communication weights of the matrix 4.2 are added to determine the communication path in the network.

$$\mathfrak{R}_d = x_i - x_j\{i \neq j\} \tag{27}$$

$$Nei_{ij} \iff \mathfrak{R}_d \leq \mathfrak{R}_C \tag{28}$$

4.2.3 Area of Coverage

The swath of the satellite is defined as the earth surface area that a satellite can see with its elevation angle at a given point of time. The swath in any distributed network depends on position, inclination, relative distance between the nodes, range of sensing and communication as shown in the Fig. 8. These parameters determines network structure and the power requirements. The coverage area changes in LEO satellites unlike GEO satellites. Thus area of coverage varies in distributed network in LEO. For the purpose of simulation we assume all the nodes to be in LEO. The temporal and spatial resolution of payload determines the area of coverage. Other factor which determines the area of coverage is the orbital velocity and the orbital plane.

Every satellite in the network has its geographical coverage area obeying the following eqs. 29, 30 and 31

$$C_{(rsensing)} = E_r\left(\arccos\left(\frac{E_r}{S_r}\right)\cos\theta - \theta\right) \tag{29}$$

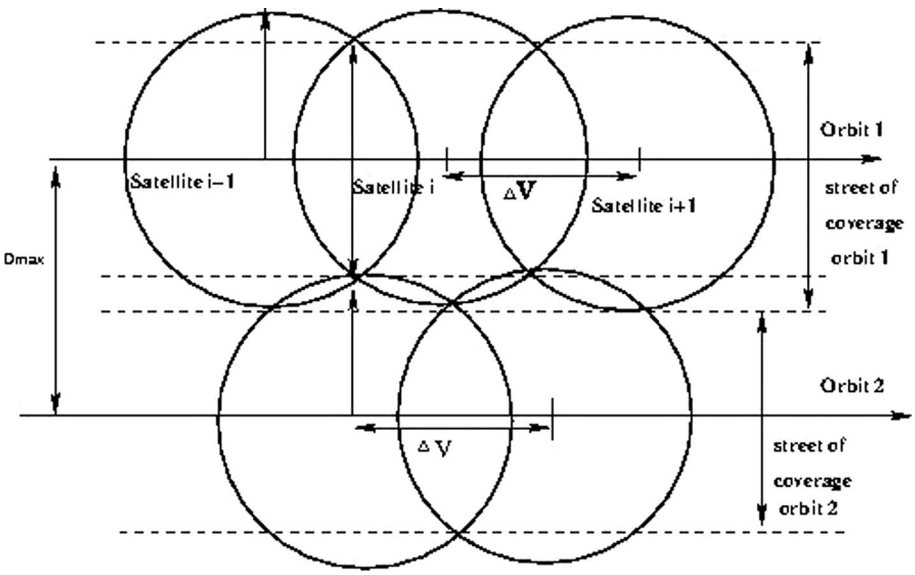

Fig. 8 Coverage area in PBNT

$$C_{(rsink)} = E_r\left(\arccos\left(\frac{E_r}{S_r}\right)\cos\theta - \theta\right) \tag{30}$$

$$(V_{(rsensing)}, V_{(rsink)}) = f(t, \theta, D_s) \tag{31}$$

where $C_{(rsensing)}$ and $C_{(rsink)}$ are the coverage area of the sink and sensing node, while E_r and S_r are earth and satellite orbit radius. θ is a elevation angle. $V_{(rsink)}$, $V_{(rsensing)}$ are the velocity of sensing nodes and sink nodes respectively. The velocity is a function of time, distance and its position. Azimuth angles are calculated using altitude of earth and the satellite. The coverage time is given by the Eq. 33

$$C_{(Nodetime)} = C_{(rsensing)} \pm \gamma E_r \tag{32}$$

$$\frac{\sin\frac{E_r}{E_r}}{\sin\phi} \tag{33}$$

where ($C_{(Nodetime)}$) indicates the coverage time and (ϕ) indicates ($\phi - Azimuthangle - \epsilon$). The coverage time of earth by sensing or sink node also depends on the communication link between the earth and the satellite and coverage time between the sensing node and the sink node.

5 Information Gathering in PBNT

Information gathering is done at node level both at $N_{sensing}$ and N_{sink} nodes. This information is sent to the ground station when sensing/sink/cluster head nodes are at perigee. In the proposed work, the Hamiltonian path is used for gathering of data from different nodes. In the proposed work, we define a graph G constructed using the set of vertices and edges as shown in the Eq. 18 to model the network. The vertices are assumed to be as sink nodes. Figure 6a shows the logical positions of the sink nodes and sensing nodes in PBNT. The main job of these nodes is to sense the data and transmit to the ground station. The sensing of the data is by two methods namely (1) Event based data gathering (2) Periodic data gathering

5.1 Event Based Data Gathering in PBNT

There are two scenarios of event based data gathering namely (1) Event Trigger by Ground Station (2) Event detection by DSBWSN.

Event Trigger by Ground Station: This is typically used during natural calamities to monitor a specific area for a particular time duration. The dynamic clusters are formed using the predetermined icosahedral pattern based on the application as shown in the Figs. 3 and 4a, b

$$C_1^m, C_2^m, C_3^m, C_4^m, C^m \ldots C_n^m \tag{34}$$

where C_n^m in Eq. 34 represent the cluster formed by $m = 1, 2, 3, 4 \ldots$ tiling pattern of icosahedral combination and $n = 1, 2, 3, \ldots$ indicates the cluster number. In the event based

model, the ground station sends commands to the cluster head. The algorithm for Event Trigger by Ground Station is described in Algorithm 2.

The steps involved in event based data gathering

Algorithm 2 Proposed Scheme for Event Trigger by Ground Station

LOOP

Select the value of m and n and send it to the particular sink node/cluster head using start command

Start command contains (*cmd*1)

(*start:C:m:n:CoverageTime:CoverageDuration:NumResolution*)

The cluster head follow the command and send a acknowledge signal to the ground station

Cluster is formed dynamically and the sensing nodes get associated to the cluster head

The cluster head and the sensing nodes sense the target location and send the data to ground station when they are at perigee (based on cluster head/sensing nodes capabilities)

Once the task is complete, the ground station sends a stop command (*cmd*2) (*stop:C:m:n*)

The cluster head stops the data gathering of the target location and resume its normal operation.

END LOOP

Event detection in DSBWSN: To increase the life time of the network, not all the nodes are active all the time. Few nodes are made active, while the rest of the nodes enter into sleep mode/power saving mode. The active nodes keep sensing the target area of the earth and a minimum computation is used to check if the event has occurred. The algorithm 3 describes Event detection in DSBWSN

Algorithm 3:

Algorithm 3 Proposed Scheme for Event detection by DSBWSN

LOOP

Let (C_n^m) be the cluster with (p) sensing nodes in the cluster.

As a part of normal operation, only few Active nodes ($A_n < p$) perform earth observation.

The Eq. 35, checks if the nodes have crossed the threshold and Eq. 36 shows if the event is detected.

If the event is detected then all the nodes in the cluster are activated and starts capturing the data of the intended target.

After a particular time span the threshold is computed again, if the event is not more existing then the node resumes its actual operation (sleep/power saving mode) if it is within the threshold value.

$$s^n = \begin{cases} 1 & (A_n \geq threshold), \\ 0 & \text{Otherwise} \end{cases} \tag{35}$$

$$ED_n = \begin{cases} Detected & if \prod_{i=1}^{q} (s^n = 1), \\ Nondetected & \text{Otherwise} \end{cases} \tag{36}$$

5.2 Periodic Sensing in PBNT for Data Gathering

In periodic data gathering process, sensing occurs for a particular span of time for capturing a specific swath of earth. Equation 37 shows periodic sensing with the interval of T, where T indicates the time duration when the node senses the target location.

$$C^{m}_{Peoridic(i)} = \begin{cases} 1 & i = 1T, 2T, 3T \ldots NT), \\ 0 & \text{Otherwise} \end{cases} \tag{37}$$

The time period is given by Eq. 38 which define the time duration when the node can cover the target location. The total time period of each node is given by T_p based on the orbital parameters. The throughput for the entire network with $N_N odes$ is given by the Eq. 39

$$T_p = t_{n+1} - t_n \tag{38}$$

$$DataThroughput = (N_N odes) * (T_p) * (Num\_Revolution\_Day) \tag{39}$$

5.3 Hamiltonian Based Data Gathering in PBNT

The data gathering is done using Hamiltonian path in the cluster from source to the destination. This is described using triangular grid graph within the cluster. The nodes inside triangle are the sensing nodes used for sensing based on the application. One complexity with this permutation of nodes getting connected depends on the permutation of nodes and the time complexity for this is given by O(N*N). The path selected for data gathering between the two nodes depends on the search for nearest neighbor. In this work, we use cycle with a minimum path within the cluster based on source to the destination cluster head/sink node using minimum hamiltonian path.

The graph is made sure that it is Hamiltonian with at least one Hamiltonian cycle and with a minimum of Hamiltonian path containing all the nodes in the graph. We also use provision for cycle extendibility when any new nodes gets added as a part of scalability. These graphs are used as it satisfies the rule of cycle extensibility. It is ensured that the degree does not exceed $n/2$. The Hamiltonian path is the best path for data gathering and aggregation in the network. Figure 7 shows cluster formation and Fig. 9 demonstrates a Hamiltonian path for the dynamic cluster.

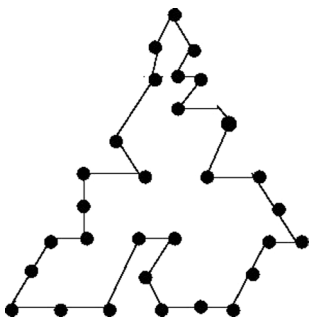

Fig. 9 Example scenario of a Hamiltonian cycle

6 Results

Deployment of satellites and testing in real time is quite expensive in space and has various legal issues. Thus a traditional way of testing the entire scenario is by using simulation. The simulation Tools used for this work include Matlab, STK, C++ and NS2. The NS2 libraries are modified to suit the space environment. This section describes the PBNT formation and information gathering using Hamiltonian path. The performance analysis of PBNT for various scenarios are discussed. The simulation results are shown in 2-D and 3-D plane for various simulation parameters listed below

- Sensing nodes weigh approximately 1 kg and sink nodes range from 1 to 10 kg.
- ISL link have data rates of 256 kbps.
- Position of the node have accuracy upto 10 cm.
- altitude ranging from 300 to 1598 km.
- Inclination ranges between 23° and 98°.
- Velocity is 7021 km/s considering LEO.
- Minimum distance between two nodes (sink–sink node or sink-sensing node or sensing–sensing node) and its relative position varies maximum of 1 km.
- Range of communication between the nodes vary from 168 to 2000 km.
- In-plane and out of plane simulation
- The inter-orbit maximum distance is considered to be 10 km
- The PBNT network was simulated using had 3–150 nodes.

6.1 PBNT Formation

The network is build with 3–150 nodes and are deployed in the Low earth orbit as shown in the Fig. 10a. The formation of fullerene comprising of both pentagonal and hexagonal faces is shown in the Fig. 10b using matlab and was further ported to STK for simulation and analysis. Figure 11a, b shows the 2D view of nodes covering the target location and Fig. 12 shows the satellite network swath of target location. These simulations shows the minimum and maximum latitudes forming the tracking loops of the nodes in the network.

6.2 Cluster Formation in the PBNT

The cluster are formed by trivalent, toroidal and spherical polyhedron is shown in the Fig. 13a using Matlab and another scenario is simulated using STK as shown in the Fig. 13b. The nodes are further activated based on the required target location using tiling pattern shown in Figs. 3 and 4a, b.

6.3 Communication Between the Satellites in the PBNT

The nodes in the network are connected with each other using inter satellite link based on the relative distance between them as given by the Eq. 27. The edges in the Fig. 10b

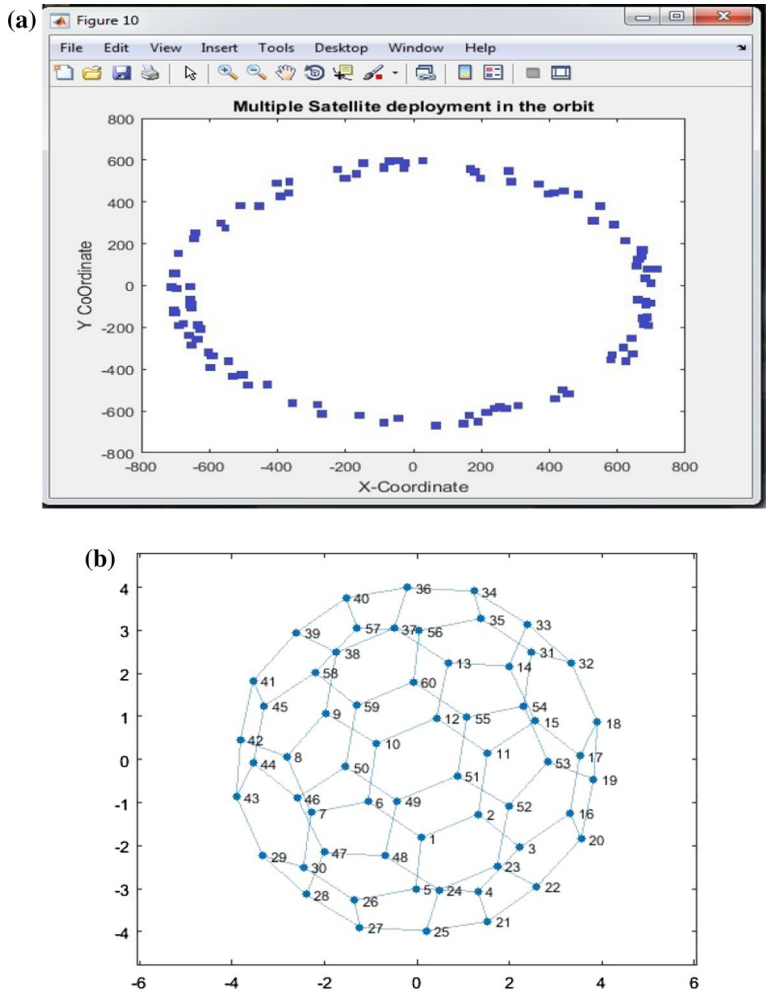

Fig. 10 **a** Nodes deployment in PBNT in low earth orbit and **b** polygon based network topology for DSB-WSN

represent the communication links between the nodes. The possible communication links is given Kronecker product and adjancency matrix helps in determining the neighbouring nodes and the corresponding links between the nodes. Figure 14 shows the adjacency matrix for the PBNT. The nodes very close to each other represent the adjacent neighbouring nodes which involve in cluster formation and help in data gathering and aggregation, while nodes far away represent isolated nodes.

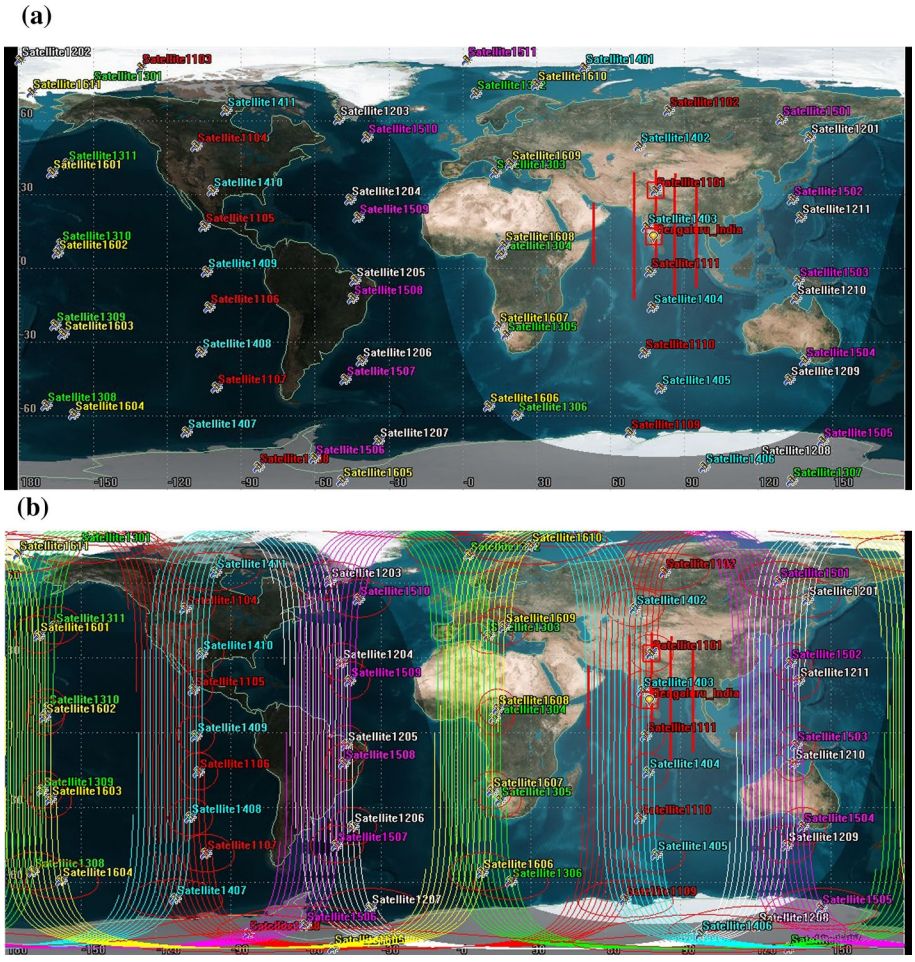

Fig. 11 **a** 2D view and **b** ground tracking of nodes of nodes in PBNT

6.4 Information Gathering

In event based data gathering initially only few nodes are active. Based on the event triggered or by the command from the ground station, the nodes gets activated. The coverage area for this scenario is shown and where a set of nodes captures the data from the target location. Figure 15a, b shows number of nodes getting increased and also enhances the coverage area of target location.

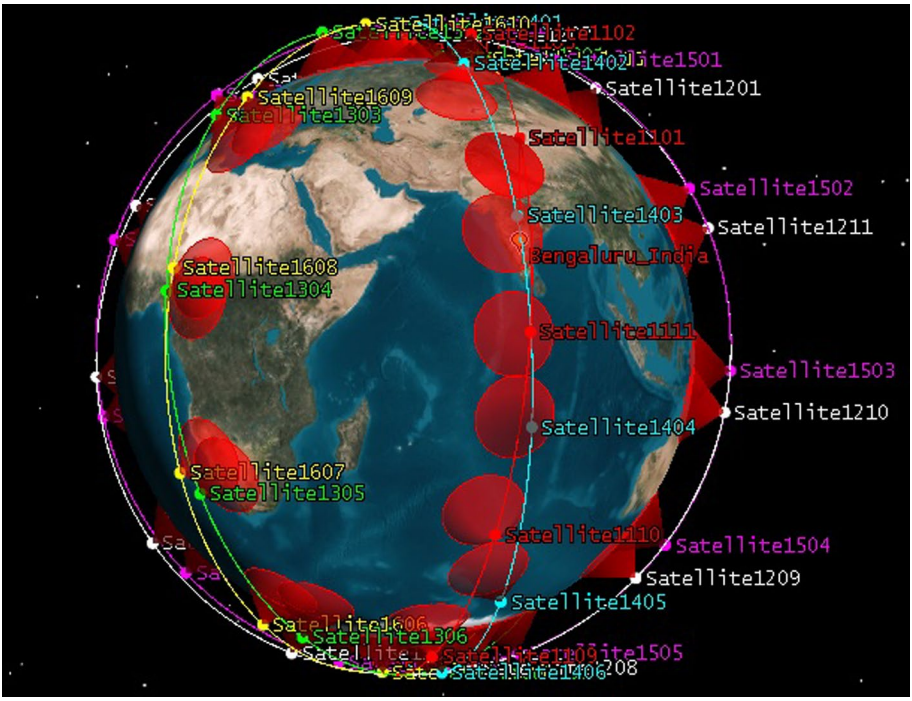

Fig. 12 Swath of target location covered by the nodes at different at different time stamps

6.5 Hamiltonian Based Data Gathering in PBNT

The fullerence takes both the pentagon shape and the hexagon shape, simulation is done considering both of the scenarios to demonstrate how the data gathering is performed using PBNT basic unit of hexagon and pentagon. The simulation shows the corresponding result showing Hamiltonian path and its logical neighbours in the Fig. 16a, b. The logical neighbour are consider for this simulation using adjacency matrix. In this example 1 the inner nodes 1, 2, 3 … 33 are the sensing nodes while the nodes 101, 102, 103, 104, 105, 106 are the sink nodes. Figure 9 shows a example scenario where the data gathering is simulated from all the nodes using Hamiltonian path. This path also forms the shortest path for gathering of data in PBNT.

Isolated nodes These are the nodes which are lying outside the defined structure or inactive nodes in the formation. The node outside the cluster and out of communication range are called isolated node. The number of isolated nodes reduces with increase in number of nodes and its communication range. Figure 17 where only few nodes from the example 1 are active and the rest of the nodes are isolated nodes.

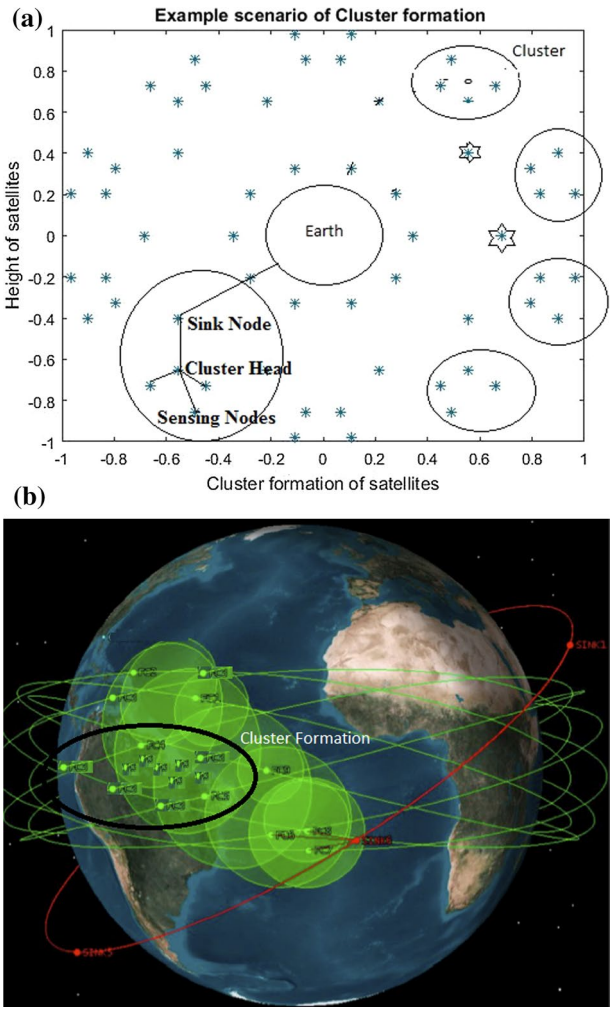

Fig. 13 Cluster formation **a** using Matlab and **b** using STK

Figure 18 shows dynamic cluster simulation with data gathering using of Hamiltonian path using the active nodes. This shows dynamic clusters at different instant of time and with different data gathering paths.

6.6 Area of Coverage

The area of coverage is simulated for various time-stamps showing the latitude and longitude of the satellite in the Fig. 11a. It shows the tracking of the satellite where the red color vertical lines represent the target location. The cone in Fig. 12 indicates the area of coverage by that satellite at that instant of time. We have considered various scenarios, one of

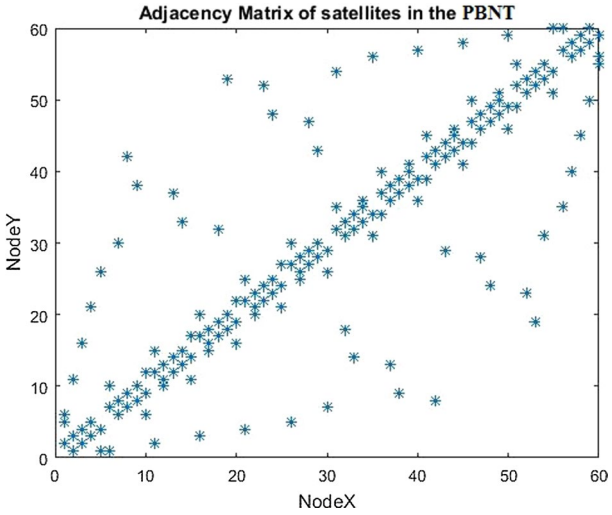

Fig. 14 Adjacency matrix of satellites in the PBTN

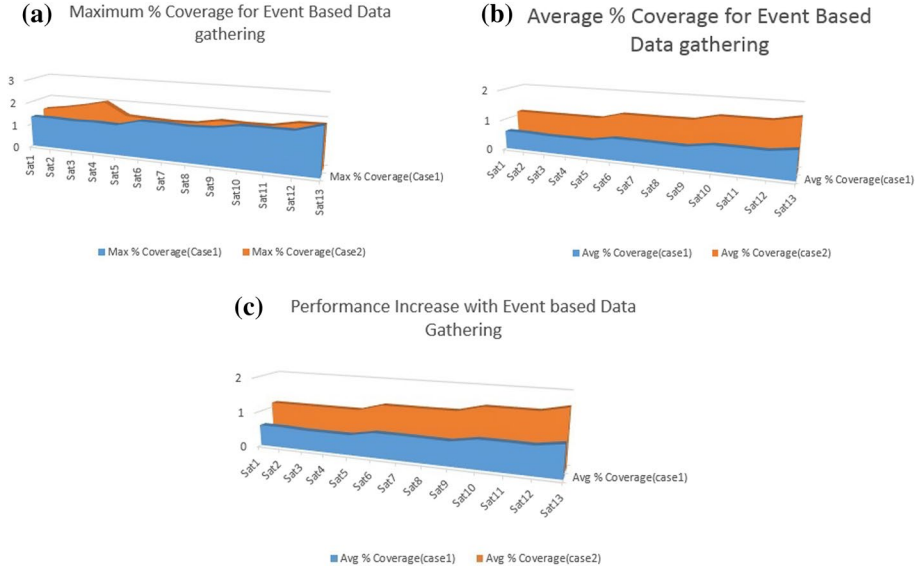

Fig. 15 Event based data gathering (**a**) and (**b**) performance analysis with event based triggering of the nodes

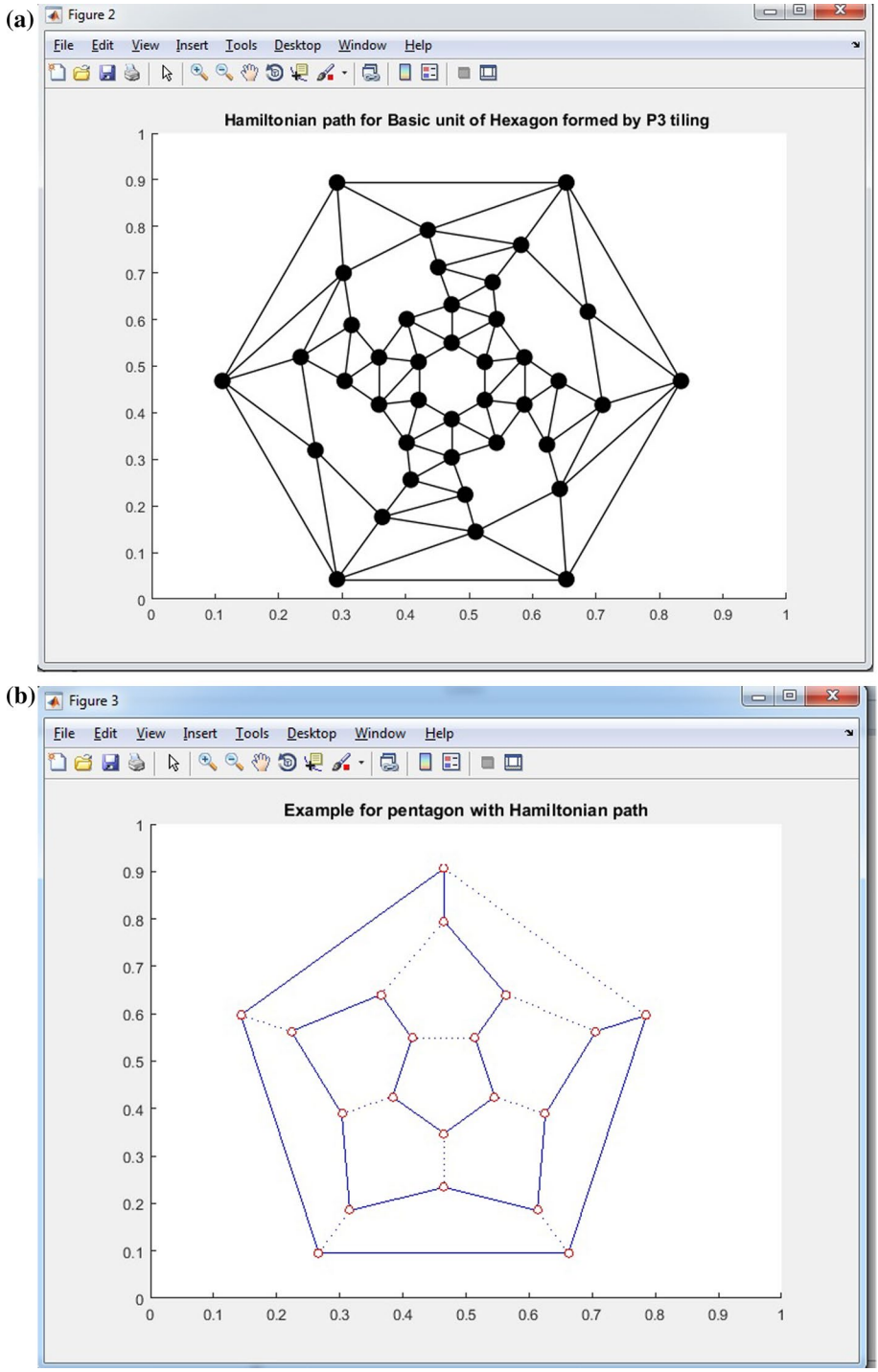

Fig. 16 Example scenario with a single cluster with sensing nodes and sink nodes (**a**) and (**b**) example scenario of only few active nodes in the cluster used for event based data gathering

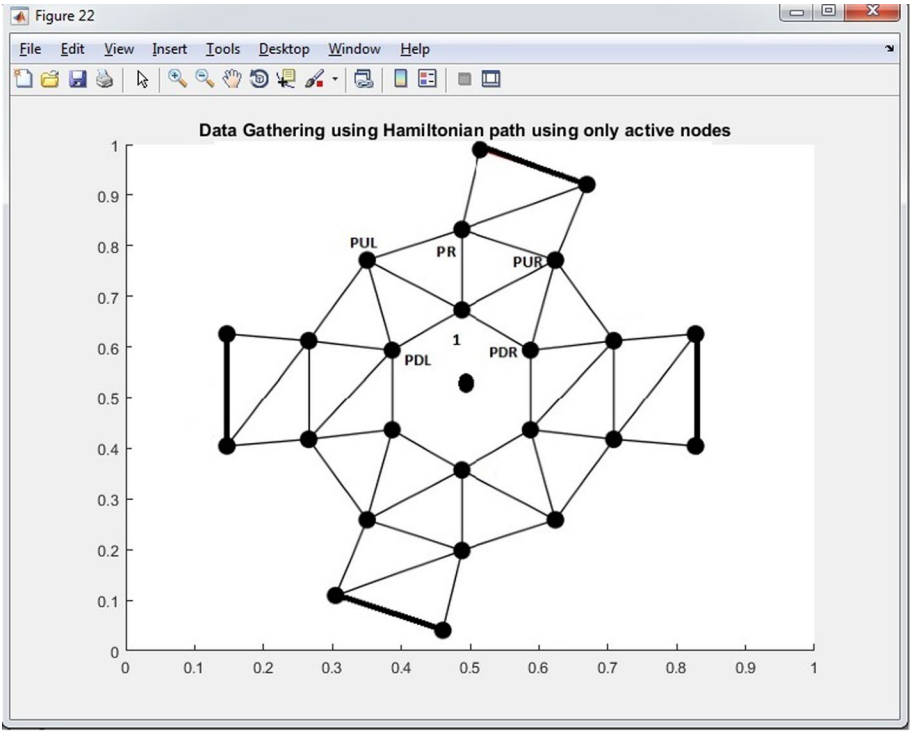

Fig. 17 Example showing Hamiltonian cycle for communication in a single cluster

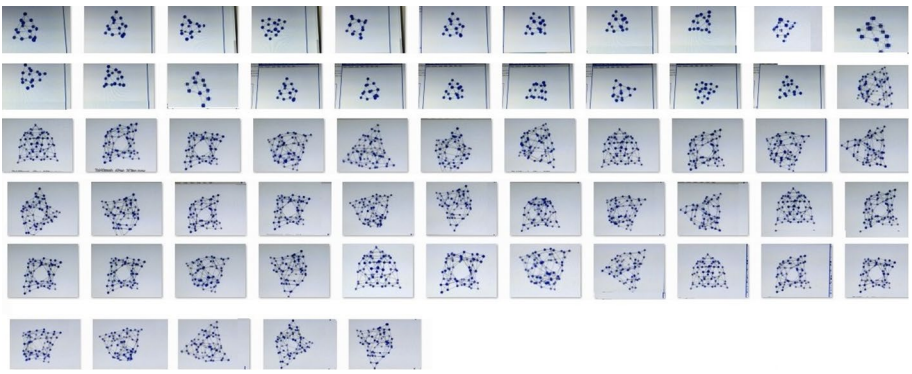

Fig. 18 Dynamic clustering of the nodes with Hamiltonian cycle in PBTN

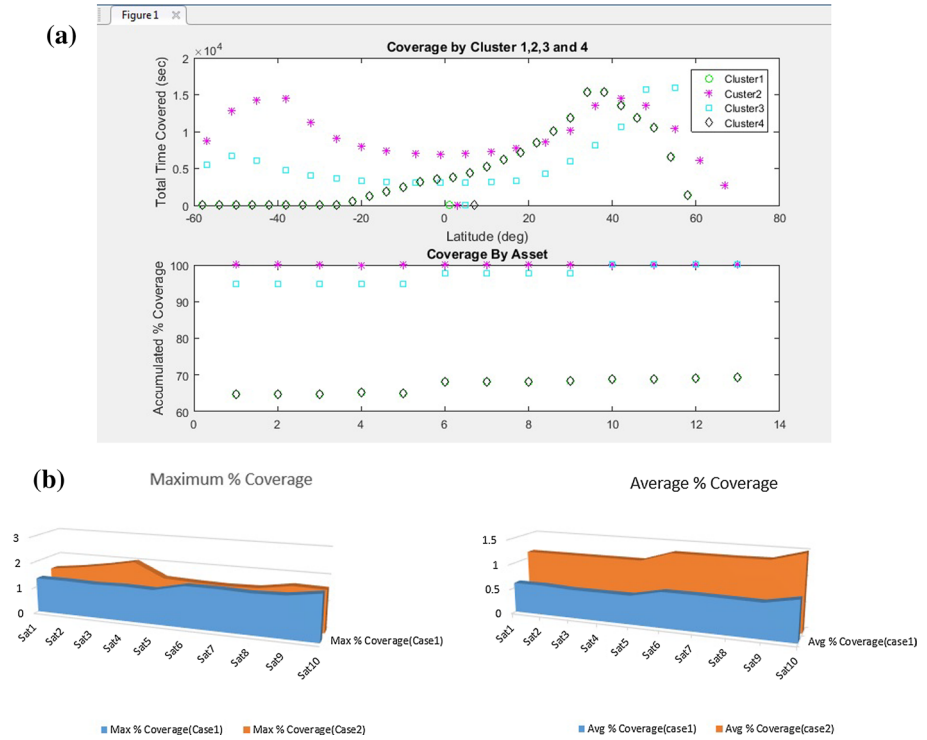

Fig. 19 Maximum percentage coverage of p3 compared to lattice structure (**a**) and (**b**) average percentage coverage of p3 compared to lattice structure

which shows a two patterns of p3 polyiamonds with inclination (45°–98°). This is used as the fundamental unit to form the icosahedral structure of PBNT. The area of coverage for this fundamental unit is analysed using coverage parameters like lattitude, assest and time duration. The analysis results are shown in Fig. 19a, b. Several other combinations of these were simulated and we see the maximum coverage is seen using these p3 polyiamonds structure compared to the lattice structure.

6.7 Communication to Ground station in the PBNT

This example shown in the Fig. 20a illustrates the duration of the nodes transferring data to the ground station. Here both the sink and the sensing nodes are considered to be communicating to the ground station. The graph Fig. 20b shows the access time of the nodes to the ground station.

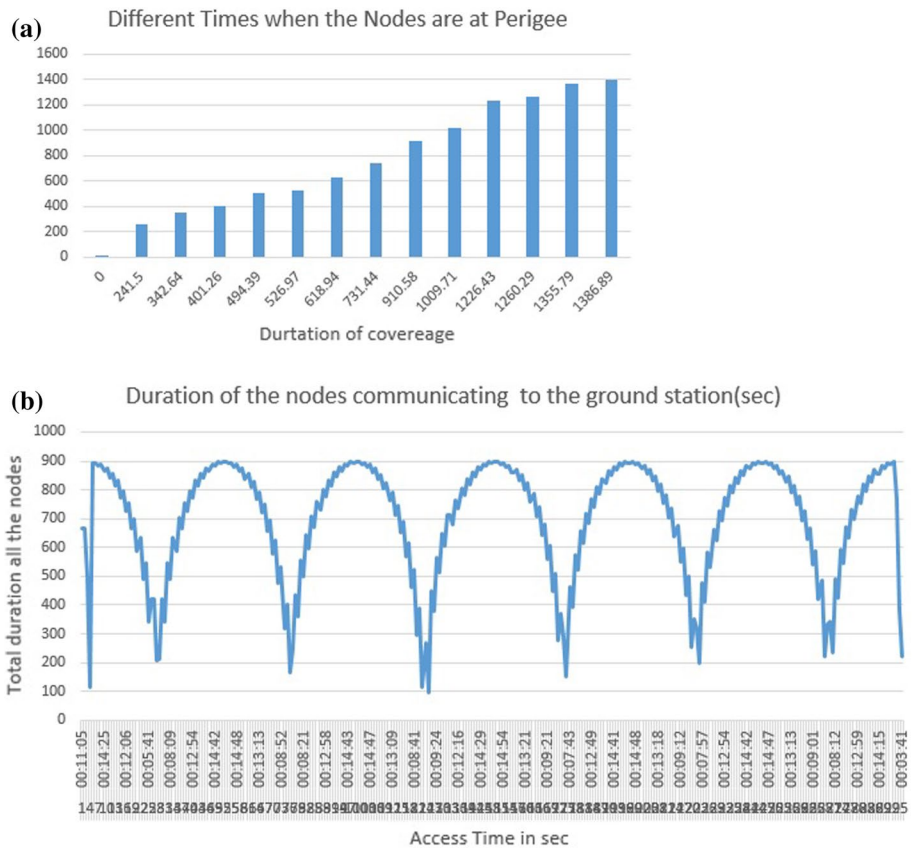

Fig. 20 Communication to ground station (**a**) and (**b**) access time and coverage duration

7 Conclusion

The main objective of this paper is to use distributed network of small satellite. The strength of any distributed network depends on the topology formation and data gathering algorithm. This paper shows the dynamic topology formation using p3 tiling and fullerence structure forming PBNT. The main objective of using hexagon or pentagon structure is that its reduces the gaps in the coverage area and helps in dynamic cluster formation. The other advantage of this network is scalability. The cluster size and shape can be dynamically changed based on field of view by making nodes active/deactive. Thus topology is dynamic and scalable. The network is reliable in case of any node failure, the nodes in the network can be reconfigured and the mission continues to work. Thus life time of the network is also increased as the network is still alive, when the node in the network fails. The second objective was event based data gathering in PBNT. The Hamiltonian path is well suited for data gathering. The event based data gathering helps in increasing the life time of the network as multiple nodes gather the data and communicates to the ground station. From the simulation we demonstrate

that multiple nodes capture the target location multiple times nodes and transmit each node(sink or sensing) transmit to the ground station unlike single large satellite. Thus we conclude that PBNT proves to be stable and efficient compared to the single large satellite. This work provides a framework for the SBWSN and this can be extended to interplanetary exploration and for scientific application.

References

1. Kuruba, P., & Sutagundar, A. V. (2017). Emerging trends of space-based wireless sensor network and its applications. In N. Kamila (Ed.), *Handbook of research on wireless sensor network trends, technologies, and applications* (pp. 35–57). Hershey, PA: IGI Global. https://doi.org/10.4018/978-1-5225-0501-3.ch002.
2. Paul, J. R. (2011). Communication platform for inter-satellite links in distributed satellite systems Doctoral dissertation, University of Surrey, UK.
3. Shcilling, K. (2011). Networked distributed pico-satellite systems for earth observation and telecommunication applications.
4. Puig-Suari, J., Turner, C., & Twiggs, R. (2001). CubeSat: The development and launch support infrastructure for eighteen different satellite customers on one launch.
5. Vladimirova, T., Bridges, C. P., Prassinos, G., Wu, X., Sidibeh, K., Barnhart, D. J., & Maynard, K. (2007). Characterising wireless sensor motes for space applications. In *Second NASA/ESA conference on adaptive hardware and systems (AHS 2007)* (pp. 43–50). IEEE.
6. Burlacu, M. M., & Lorenz, P. (2010). A survey of small satellites domain: Challenges, applications and communications key issues.
7. Wang, J., Li, L., & Zhou, M. (2007). Topological dynamics characterization for LEO satellite networks. *Computer Networks*, *51*(1), 43–53.
8. Draim, J. E., Cefola, P., & Castrel, D. (2000). Elliptical orbit constellations a new paradigm for higher efficiency in space systems. In *2000 IEEE aerospace conference. Proceedings (Cat. No. 00TH8484)* (Vol. 7, pp. 27–35). IEEE.
9. Wood, L. (2001). Internetworking with satellite constellations. Doctoral dissertation, University of Surrey.
10. Christopher, P. (2009). Molniya system alternatives for geostationary satellite systems with applications to 72–100 GHz systems. In *Proceedings Ka broadband conference* (pp. 1–9).
11. Taormina, F. A. (1997). *Application of Hughes Communications, Inc. for authority to launch and operate Spaceway NGSO, an NGSO expansion to the Spaceway global broadband satellite system*. Filing with the US Federal Communications Commission, Hughes Communications, Inc, 22.
12. Elizondo, E., Gobbi, R., Modelfino, A., & Gargione, F. (1997). Evolution of the Astrolink system. In *17th AIAA international communications satellite systems conference and exhibit* (p. 1208).
13. Vladimirova, T., Bridges, C. P., Paul, J. R., Malik, S. A., & Sweeting, M. N. (2010). Space-based wireless sensor networks: Design issues. In *2010 IEEE aerospace conference* (pp. 1-14). IEEE.
14. Tafazoli, M. (2009). A study of on-orbit spacecraft failures. *Acta Astronautica*, *64*(2–3), 195–205.
15. Boiardt, H., & Rodriguez, C. (2009). The use of Iridium's satellite network for nanosatellite communications in low earth orbit. In *2009 IEEE aerospace conference* (pp. 1–5). IEEE.
16. Mortari, D., & Wilkins, M. P. (2008). Flower constellation set theory. Part I: Compatibility and phasing. *IEEE Transactions on Aerospace and Electronic Systems*, *44*(3), 953–962.
17. Davis, J. J., Avendaño, M. E., & Mortari, D. (2013). The 3-D lattice theory of flower constellations. *Celestial Mechanics and Dynamical Astronomy*, *116*(4), 339–356.
18. Stephens, P., Cooksley, J., da Silva Curiel, A., Boland, L., Jason, S., Northham, J., & Machin, S. (2003). Launch of the international disaster monitoring constellation; The development of a novel international partnership in space. In *Proceedings of international conference on recent advances in space technologies, 2003. RAST'03.* (pp. 525–535). IEEE.
19. Xiang, W., & Jørgensen, J. L. (2005). Formation flying: A subject being fast unfolding in space. In *5th IAA symposium on small satellites for earth observation*.
20. Presti, D., Herman, J., & Codazzi, A. (2004). Mission operations system design and adaptations for the twin-satellite mission GRACE. In *Space OPS 2004 conference* (p. 219).
21. Chen, Z., & Zeng, Y. (2013). A swarm intelligence networking framework for small satellite systems. *Communications and Network*, *171*, 171–175.

22. Yeh, H. H., & Sparks, A. (2000). Geometry and control of satellite formations. In *Proceedings of the 2000 American control conference. ACC (IEEE Cat. No. 00CH36334)* (Vol. 1, No. 6, pp. 384–388). IEEE.
23. Nag, S., & Summerer, L. (2013). Behaviour based, autonomous and distributed scatter manoeuvres for satellite swarms. *Acta Astronautica*, *82*(1), 95–109.
24. Martin, M., Klupar, P., Kilberg, S., & Winter, J. (2001). Techsat 21 and revolutionizing space missions using microsatellites.
25. Navabi, M., Barati, M., & Bonyan, H. (2013). Algebraic orbit elements difference description of dynamics models for satellite formation flying. In *2013 6th international conference on recent advances in space technologies (RAST)* (pp. 277–280). IEEE.
26. Barth, D., & Raspaud, A. (1994). Two edge-disjoint Hamiltonian cycles in the butterfly graph. *Information Processing Letters*, *51*(4), 175–179.
27. Guojun, L., & Chuanping, C. (1999). Disjoint Hamiltonian cycles in graphs. *Australasian Journal of Combinatorics*, *19*, S3–S9.
28. Gorbenko, A., & Popov, V. (2012). The problem of finding two edge-disjoint Hamiltonian cycles. *Applied Mathematical Sciences*, *6*(132), 6563–6566.

Mrs. Padmaja Kuruba holds a Bachelor degree in Electronics and Communication Engineering and Master in Technology in Digital Electronics. She has over 18 years of experience including Industry and Academia. She has worked with Larsen and Tubro (L&T) InfoTech, Cisco system, Mindtree Limited and Kyocera Wireless Limited. She has worked at Jain University Bengaluru and currently is associated with Global Academy of Technology Bengaluru. Her area of research includes Wireless Communication (LTE and Wimax), Wireless Sensor Networks, Satellite Communication. She has been awarded with Excellent Performer Award at L&T (Larsen and Tubro InfoTech) for LTE Project, Shining Star award from Mindtree, Certified with 'A' Grade for Wireless and Mobile Communication at Indian Institute of Science (IISC) Bengaluru. She has filed a Patent on Navigation System. She is Recognized as Scientific Researcher. She was designated as Board of Examination at Jain University. She has won prizes at several National and State Level Project Competition. She is also a Resource person at National Level, Faculty Development Programs. She has contributed to the research field by authoring few conference and journal papers. She has also authored a Book Chapter in "Handbook of Research on Wireless Sensor Network Trends, Technologies, and Applications".

N. D. Dushyantha holds a M.Tech degree and a Ph.D in Electronics and Communication Engineering. He is currently a professor at K S School of Engineering and Management, Bangalore, His research interests include Speech processing, Machine learning, Deep learning. He is author or co-author of over 20 international journal papers or conference proceedings.

Affiliations

Padmaja Kuruba[1] · N. D. Dushyantha[2]

✉ Padmaja Kuruba
padmajamtech@gmail.com

N. D. Dushyantha
dushyanth_crp@rediffmail.com

[1] Department of Electronics and Communication Engineering, Global Academy of Technology, Bengaluru 560098, India

[2] Department of Electronics and Communication Engineering, K S School of Engineering and Management, Bengaluru 560062, India